

Solar Radiation Measurement Tools and Their Impact on In Situ Testing A Portuguese Case Study

Oliveira, Marta; Silva Lopes, Hélder; Mendonça, Paulo ; Tenpierik, Martin; Torres Silva, Lúcia

DOI

[10.3390/buildings14072117](https://doi.org/10.3390/buildings14072117)

Publication date

2024

Document Version

Final published version

Published in

Buildings

Citation (APA)

Oliveira, M., Silva Lopes, H., Mendonça, P., Tenpierik, M., & Torres Silva, L. (2024). Solar Radiation Measurement Tools and Their Impact on In Situ Testing: A Portuguese Case Study. *Buildings*, 14(7), Article 2117. <https://doi.org/10.3390/buildings14072117>

Important note

To cite this publication, please use the final published version (if applicable).
Please check the document version above.

Copyright

Other than for strictly personal use, it is not permitted to download, forward or distribute the text or part of it, without the consent of the author(s) and/or copyright holder(s), unless the work is under an open content license such as Creative Commons.

Takedown policy

Please contact us and provide details if you believe this document breaches copyrights.
We will remove access to the work immediately and investigate your claim.

Article

Solar Radiation Measurement Tools and Their Impact on In Situ Testing—A Portuguese Case Study

Marta Oliveira ^{1,*}, Hélder Silva Lopes ², Paulo Mendonça ³, Martin Tenpierik ⁴ and Lígia Torres Silva ⁵

- ¹ Centre for Territory, Environment and Construction (CTAC), Department of Civil Engineering, Engineering School, University of Minho, 4800-058 Guimarães, Portugal
- ² Lab2PT—Landscape, Heritage and Territory Laboratory, Department of Geography, University of Minho, 4800-058 Guimarães, Portugal; helderlopes@geografia.uminho.pt
- ³ Lab2PT—Landscape, Heritage and Territory Laboratory, School of Architecture, Art and Design, University of Minho, 4800-058 Guimarães, Portugal; mendonca@aad.uminho.pt
- ⁴ Faculty of Architecture and the Built Environment, Delft University of Technology, 2628 Delft, The Netherlands; m.j.tenpierik@tudelft.nl
- ⁵ Centre for Territory, Environment and Construction (CTAC), School of Engineering, University of Minho, 4800-058 Guimarães, Portugal; lsilva@civil.uminho.pt
- * Correspondence: marta.arq@hotmail.com

Abstract: Accurate knowledge of solar radiation data or its estimation is crucial to maximize the benefits derived from the Sun. In this context, many sectors are re-evaluating their investments and plans to increase profit margins in line with sustainable development based on knowledge and estimation of solar radiation. This scenario has drawn the attention of researchers to the estimation and measurement of solar radiation with a low level of error. Various types of models, such as empirical models, time series, artificial intelligence algorithms and hybrid models, for estimating and measuring solar radiation have been continuously developed in the literature. In general, these models require atmospheric, geographical, climatic and historical solar radiation data from a specific region for accurate estimation. Each analysis model has its advantages and disadvantages when it comes to estimating solar radiation and, depending on the model, the results for one region may be better or worse than for another. Furthermore, it has been observed that an input parameter that significantly improves the model's performance in one region can make it difficult to succeed in another. The research gaps, challenges and future directions in terms of solar radiation estimation have substantial impacts, but regardless of the model, in situ measurements and commercially available equipment consistently influence solar radiation calculations and, subsequently, simulations or estimates. This article aims to exemplify, through a case study in a multi-family residential building located in Viana do Castelo, a city in the north of Portugal, the difficulties of capturing the spectrum of radiations that make up the total radiation that reaches the measuring equipment or site. Three pieces of equipment are used—a silicon pyranometer, a thermopile pyranometer and a solar meter—on the same day, in the same place, under the same meteorological conditions and with the same measurement method. It is found that the thermopile pyranometer has superior behavior, as it does not oscillate as much with external factors such as the ambient temperature, which influence the other two pieces of equipment. However, due to the different assumptions of the measurement models, the various components of the measurement site make it difficult to obtain the most accurate and reliable results in most studies. Despite the advantages of each model, measurement models have gained prominence in terms of the ease of use and low operating costs rather than the rigor of their results.

Keywords: solar radiation; measurement equipment; Viana do Castelo; environment impact; measurement uncertainty



Citation: Oliveira, M.; Silva Lopes, H.; Mendonça, P.; Tenpierik, M.; Silva, L.T. Solar Radiation Measurement Tools and Their Impact on In Situ Testing—A Portuguese Case Study. *Buildings* **2024**, *14*, 2117. <https://doi.org/10.3390/buildings14072117>

Academic Editor: Danny Hin Wa Li

Received: 23 May 2024

Revised: 24 June 2024

Accepted: 1 July 2024

Published: 10 July 2024



Copyright: © 2024 by the authors. Licensee MDPI, Basel, Switzerland. This article is an open access article distributed under the terms and conditions of the Creative Commons Attribution (CC BY) license (<https://creativecommons.org/licenses/by/4.0/>).

1. Introduction

The solar radiation that penetrates the atmosphere and reaches the Earth's surface is vital for the chemical, physical, and biological processes necessary for sustaining life [1–3]. Variations in solar radiation directly affect climate data, the hydrological cycle, sensible and latent heat, evaporation, ecological systems, migration patterns, and other crucial parameters [1,4,5]. In addition to these critical aspects, solar energy has a significantly lower environmental impact compared to traditional energy sources such as fossil fuels. Due to all these characteristics, solar energy systems are expected to play a fundamental role in mitigating carbon emissions and harnessing solar radiation, especially in developing countries [4]. Solar energy is progressively being regarded as one of the most vital renewable and sustainable energy sources for tackling the global energy crisis [6].

Countries that rely on solar systems have experienced immediate economic and environmental benefits, leading them to increase investment in solar power plants and rethink their energy strategies based on their solar energy potential, such as electricity production. A country's potential for solar power can easily be gauged by its solar radiation levels. Regions with high solar energy potential include Africa, Australia, South America, Southern Europe, and Asia, particularly India. In these areas, solar energy is frequently used for electricity and heat production. Conversely, in regions with lower solar energy potential, the use of concentrated solar systems is considered a practical solution to boost solar radiation potential [7].

With current technology, solar energy can be harnessed through various methods, including solar thermal electricity generation, solar heating systems, and photovoltaic cells (PV systems). Of these methods, photovoltaic solar systems are widely used globally, providing an easy and efficient way to generate electricity [8].

There has been a substantial global shift toward solar energy. The reason why countries are showing significant growth in their interest in solar energy is to ensure economic sustainability by gradually reducing dependence on fossil fuels. Since the Brundtland Report, the concept of sustainable development has emerged, which aims to promote changes in environmental quality, economic development and social structure to benefit present and future generations. It was in this context that the need for society to commit to a more sustainable lifestyle became evident (World Commission on Environment and Development, 1987) [9]. International agreements, such as the Paris Agreement (an attempt to effectively combat climate change by reducing greenhouse gas (GHG) emissions and defining the Sustainable Development Goals for 2030), the Kyoto Protocol (which portrays a considerable increase in concerns about sustainability and the setting of targets) and other proposals aimed at reducing the energy intensity of cities are shown in Figure 1.

Growing recognition of urbanization reflected in global frameworks for sustainable global development.

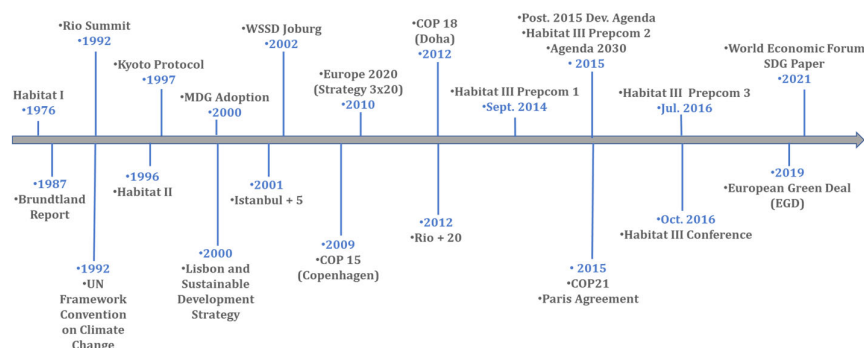


Figure 1. The evolution of the global development framework for sustainable development.

While solar energy has proved to be a highly valuable source of renewable energy, the electricity production capacity of PV modules largely depends on solar radiation, the climate of the solar park location, and the meteorological conditions [4,5,10,11]. With the increasing installation of photovoltaic systems worldwide, it becomes crucial to estimate

the solar radiation reaching the Earth and the power obtained from these systems. This way, it is possible to determine investment costs and achieve grid integration [1–3,12].

The International Energy Agency's (IEA's) Renewables 2021 report predicted a record increase in the capacity of renewable energy sources driven by photovoltaic systems in 2021. Countries expanding their photovoltaic solar energy production have addressed energy security concerns and the volatility of fossil fuel prices. The report projected continued growth in the coming years, with nearly 290 gigawatts (GW) of new renewable energy commissioned in 2021, a 3% increase from 2020. Photovoltaic systems accounted for more than half of the renewable energy expansion in 2021, followed by wind and hydroelectric power [5,13].

To create a future perspective for a solar energy system to be established in each region, it is necessary to measure the solar radiation values of the region to determine the solar energy potential of that specific geographical area. Solar radiation estimation provides essential information not only for the installation of solar energy systems but also for reliable grid operation, as the stochastic nature of solar radiation, mainly caused by cloud shadow movement between the Sun and, for example, photovoltaic panels, induces significant, sudden, and unexpected fluctuations in the power output of PV modules [14]. The variability of solar photovoltaic systems' energy poses a serious challenge to energy companies and transmission system operators, and accurate load estimates [15] and measurement equipment are of great importance [10].

Various models and methods have been developed to estimate solar radiation data with the least possible error. However, most of them use data obtained through in situ measurements, which exhibit significant variability in capturing solar radiation.

Data related to solar radiation were initially obtained through empirical mathematical models. Once the importance of solar radiation data was recognized, they became widely used in many critical sectors, such as agriculture, energy production, tourism, etc. In this context, many studies have attempted to estimate solar radiation data using different input parameters, namely cloud cover, rainfall, sky coverage, ambient temperature, dew point, air pressure, extraterrestrial radiation, latitude, relative humidity, longitude, sunshine duration, solar azimuth and day length [5].

Most input parameters generally consist of environmental and ecological parameters. Since solar radiation is a time-dependent variable, some studies have included data such as hours, days, months, and years in their algorithms for the testing phases. However, a notable number of researchers also consider solar radiation values as location-dependent variables, incorporating geographically significant data (such as latitude, longitude, altitude, and region elevation) in addition to environmental and ecological input parameters.

The attempt to define limits based on the use of various parameters and equipment has proved to be highly useful. Numerous studies recommend various methods for estimating radiation fluxes, relying on a multitude of parameters such as the air temperature, air humidity (HR-%), cloud cover, time of day, and day of the year [16–18]. However, the surface albedo (α) and proportions of the angle of incidence (β) must be specified in these models. Additionally, other factors should be considered, such as the geometric properties of buildings, vegetation, reflection properties, and surface roughness. For the application of these models in simple situations, it is crucial to consider the following radiation fluxes:

1. Direct short-wavelength (λ) radiation colliding with the sunlit portion of the body.
2. Diffuse short- λ radiation originating from the sky because of scattering and ground reflection.
3. Long- λ radiation emitted by the sky fraction and the ground.
4. Reflected short- λ radiation, controlled by the albedo of the clothed body.
5. Long- λ radiation emitted based on the surface temperature.
6. Heat loss by convection through sensible and latent heat exchange with the air, partially modeled by the wind speed.
7. Heat exchange by physical conductivity with the ground.

Over the years, a significant amount of research, development, and innovation in solar radiation measuring equipment has been required to improve the measurement and/or the calibration standards and provide suggestions for improvement. Table 1 lists studies that were conducted over time in an effort to reduce acquisition prices, improve measuring capabilities, test various cell types, and create solar capture sensors. All had the goal of increasing, researching, and learning about different instruments that can be used to collect data, detect errors, achieve accuracy, amplitude, and regulate outcome uncertainty.

Table 1. Studies of alternative solar radiation measurement equipment.

Studies	Resume
Nollas et al. (2023) [19]	Quality control procedure for 1 min pyranometric measurements of global and shadow band-based diffuse solar irradiance, according to the Köppen–Geiger classification system.
Lorenz et al. (2022) [20]	High-resolution measurement network of global horizontal and tilted solar irradiance using a pyranometer, measuring global horizontal irradiance, and three silicon cells with different orientations.
Mudike (2021) [21]	The study presents the actual field results from a calibration procedure of reference solar radiometers using an absolute cavity radiometer (ACR).
Mohammad et al. (2020) [22]	Direct normal irradiation (DNI) and global solar radiation measurement instruments were used and the global solar radiation data from the two devices were compared.
Moiz et al. (2020) [23]	A silicon nanowire-based hybrid solar cell (SiNW) study.
Lillo-Bravo et al. (2020) [24]	This model, is based on the characterization of the relation between the data measured with a thermopile pyranometer and a calibrated cell as a function of the sky condition and the solar elevation.
Tejada et al. (2020) [25]	In the study, a low-cost pyranometer is developed to detect solar irradiance by utilizing a Peltier cell (TEC-12705) as a thermoelectric generator.
John et al. (2019) [26]	An electronic pyranometer approach for measuring solar radiation.
Azouzoute (2019) [27]	This study evaluates the difference between the existing two devices used in the PV market such as thermopile pyranometer and reference cell.
Tohsing et al. (2019) [28]	A measuring broadband solar irradiance study using a pyranometer and phototransistors as a light detector.
Osinowo et al. (2019) [29]	A study that developed an instrument (photodiode device), a low-cost pyrometer, utilizing “locally sourced materials”.
Rus-Casas et al. (2019) [30]	This research presents an IoT-connected electronic device able to measure global radiation in photovoltaic applications.
Vignola et al. (2019) [31]	Up-to-date review of the important aspects of solar and infrared radiation measurements: radiometer design; equipment installation, operation, maintenance, and calibration; data quality assessment parameters.
Barros et al. (2018) [32]	Proposes a low-cost solution that monitors sun irradiance using conventional meters. An LDR sensor calibration was performed using a photodiode pyranometer.
Avallone et al. (2018) [33]	Compares thermal devices and radiation sensors used for measuring sun radiation. An elementary and low-cost version of thermal pyranometers was examined, built, and fabricated to determine their efficiency.
López-Lapeña (2018) [34]	A solar energy radiation measurement study with a low-power solar energy harvester.
Awasthil and Poudyal (2018) [35]	A daily global solar radiation (GSR) study using an CMP6 pyranometer.
Vignola et al. (2018) [36]	Compare the efficiency of photodiode-based pyranometers with reference solar cells on fixed and tracking surfaces.
Orsetti et al. (2016) [37]	Proposes a new cost-effective sensor and algorithm for tracking and measuring sun irradiance using photovoltaic cells and a digital sensor interface.

Table 1. Cont.

Studies	Resume
Michalsky et al. (2017) [38]	A study that analyses improvements in pyranometer nighttime offsets using high-flow DC ventilation.
Parthasarathy and Anandkumar (2016) [39]	In this study using photo diodes, signal conditioning, and amplification, a low-cost pyranometer for measuring solar irradiation was built.
Chaiyapinunt et al. (2016) [40]	A shadow-ring device is developed for use with a pyranometer to measure diffuse solar radiation incident on a vertical surface.
Agawa and Ibrahim (2016) [41]	A study on “Development of Micro Controller-Based Monitoring System for a Stand-Alone Photovoltaic System”.
Nwankwo and Nnabuchi (2015) [42]	A study where a pyranometer was constructed using a silicon photodiode.
Olano et al. (2015) [43]	Several calibration coefficient results have been analyzed in order to validate different methodologies. Measurement is directly influenced by the reference calibration coefficient and uncertainty of the field pyranometer used.
Srikrishnan (2015) [44]	Applies artificial neural networks to estimate DNI from the irradiance measurements of numerous pyranometers.
Dumitrescu et al. (2015) [45]	Using a professional pyranometer as a reference, this study developed an electronic equipment-based pyranometer for broadband irradiance measurements and calibrated the prototype device.
Menyhart et al. (2015) [46]	The authors believe that it is possible to control the quality of solar measurement data by optimizing the levelling of the pyranometer sensor location.
Fuentes et al. (2014) [47]	Solar radiation is measured using a silicon-cell pyranometer. A study was conducted to design a microcontroller-based data gathering system for a distant PV facility.
Daniel and Odinakach (2014) [48]	A study that uses a little rectangular silicon photocell as the sensor and digital solar radiation meter for measuring solar radiation was designed, built, and calibrated.
Hidalgo et al. (2013) [49]	A study based on using the phototransistor with low-cost components, design an affordable sensor (pyranometer) to measure solar irradiance.
Hafid et al. (2014) [50]	A study based on the use of a Peltier effect thermopile as a pyranometer for large-spectrum measurements. Using graphite material on one side to maximize solar radiation absorption.
Baltazar et al. (2014) [51]	Methodology to estimate the normal incident solar radiation based on an anisotropic clear sky model using a multi-pyranometer array (MPA).
Geuder et al. (2014) [52]	Demonstrates that the pyranometer measurement suffers from an annual deviation of 2% and suggests that calibration should be per-formed every 2 years and the RMSE should be reduced to 2%.
Patil et al. (2013) [53]	Investigates the development of lower-cost devices (photodiode-based pyranometers) capable of competing with standard thermopile-based pyranometers in measuring solar irradiance or solar radiation flux density in the visible spectral range.
Awasthi and Mor (2012) [54]	A study with innovative technology that allows real-time sun radiance data to be monitored via a local area network (LAN) or the Internet, employing a radiometer with analogue circuits for signal preprocessing from solar cells.
Nwankwo et al. (2012) [55]	A study of a locally built pyranometer for sensing global solar radiation, calibrated with the Einstrain lung pyranometer model.
Medugu et al. (2010) [56]	The dependable model pyranometer was developed as a piece of sun radiation-measuring equipment. The sensor element is made up of a silicon diode set on a plastic base and a Teflon diffuser.
Macome et al. (2009) [57]	The study aims to design, build, and characterize a multi-sensor sun radiation detector that evaluates the use of a weighted combination of photodiode measurements with a rotating shadow band to simultaneously monitor diffuse and beam solar radiation.
Martínez et al. (2009) [58]	The investigation involves the design, creation, and test of a new pyranometer for measuring global sun irradiance or flux density within the visible spectral range.

Table 1. Cont.

Studies	Resume
Gueymard and Myers (2009) [59]	This contribution evaluates the impact of instrument uncertainties contributing to data inaccuracies and their effect on short-term and long-term measurement series, and on radiation model validation studies.
Lester (2006) [60]	This study proposes a method to find an RS function to model a pyranometer's changing RS (the signal-to-irradiance ratio is the responsivity (RS) of the instrument [$RS = \text{signal}/\text{irradiance} = \text{microvolts}/(W/m^2)$]).
Okonkwo and Onwuala (2002) [61]	The study was developed around a phototransistor and compared to a typical equipment that used an integrated pyranometer model to measure radiation.
Beaubien et al. (1998) [62]	A study analyzed and assessed three varieties of thermal-converting pyranometers (black surface): two designs use diffusing front-optics, and the third uses standard double-domed enclosures. The study looked at three temperature measurement techniques: thin-film bismuth antimonide thermopiles, bismuth telluride thermopiles, and platinum resistance thermometers (PRTs).
Soulayman (1995) [63]	A method that proposes to considerably reduce the high errors normal in solar radiation data obtained by actinographs or by non-calibrated Eppley-type pyranometers.

Studies of alternative solar radiation measurement equipment to the standard ones (thermopile pyranometer, photodiode pyranometer and photovoltaic pyranometer) but which were intended to make solar radiation measurements feasible, whether they complied with the ISO standards or WMO requirements, but with the purpose of establishing the precision, range, amplitude, uncertainty and error.

The primary objective of this paper is to improve the accuracy of solar radiation measurement estimation by using various parameters as input data for predicting solar radiation through the analysis of various instruments. It is recognized that these predictions may not always be feasible or completely accurate. Depending on the circumstances and performance conditions of solar radiation estimation models, high-performance estimates using a smaller dataset may prove to be more crucial. In this sense, the proposed Portuguese case study aims to present an example of in situ measurements, with different measuring instruments and with similar levels of precision, but the results obtained do not demonstrate this similarity.

Then, this study aims to scrutinize the key equipment used for real data collection, specifically the in situ solar radiation measurement instrument. All the estimation models, whether conventional (empirical, mathematical models, etc.) or innovative approaches based on artificial intelligence (machine-learning approaches, hybrid models, etc.), rely on this instrument as the basis for their simulations [14,64]. The purpose of this study is to provide a comparative analysis of the different measurement tools (from three selected devices).

2. Solar Radiation Measurement Instruments

Solar radiation can be evaluated according to the type of radiation measured, which in turn gives rise to different equipment names. The solar radiation reaching a specific point on the Earth is called direct and diffuse radiation.

Radiometers are instruments that can measure any form of radiation. Pyrheliometers and pyranometers are two forms of radiometers that measure solar irradiation. Pyranometers measure numerous components of radiation and are distinguished by their capacity to detect solar radiation from diverse locations in the sky. Pyrheliometers measure DNI (direct normal irradiance), whereas pyranometers measure GHI (global horizontal irradiance), DHI (diffuse horizontal irradiance), or POA (plane-of-array) irradiance. The global solar pyranometer is a common instrument for measuring sun irradiance's combined direct and diffuse components.

Solar radiation is the radiant energy that comes from the Sun and propagates in the form of short electromagnetic waves in all directions. However, it is noteworthy that part of this radiation may be absorbed, scattered, or reflected as it traverses the Earth's atmosphere. Thus, only a portion of the total solar radiation reaches the Earth's surface in the form of two components: direct radiation (the part that passed freely through the atmosphere) and diffuse radiation (the part that was scattered by the atmosphere), whose sum is designated as global radiation and can be calculated by Equation (1) or the equivalent Formula (2) from Ameen et al. (2019) [65].

$$E_{g\downarrow} = E \times \cos(\theta) + E_d \quad (1)$$

where E is direct radiation, E_d is diffuse radiation, θ is the angle between the surface normal and the position of the Sun in the sky and the calculation provides the total available amount of solar energy on the Earth's surface, the global irradiance E_g .

The measurable radiation, according to Ameen et al. (2019) [65], on a horizontal surface is referred to as global horizontal irradiance (GHI). The direct solar beam passing through the atmosphere is referred to as direct normal irradiance (DNI), and diffuse horizontal irradiance (DHI) is a type of solar irradiance in which particles and molecules (such as clouds or dust) in the Earth's atmosphere scatter solar radiation [66]. The relationship between the components of solar irradiance can be calculated by Ameen et al.'s formula (2019) [65], where θ indicates the angle of incidence (Equation (2)):

$$GHI = DNI \times \cos(\theta) + DHI \quad (2)$$

The sum of these two radiations is also known as global solar radiation, and pyranometers are the radiometers that measure global solar radiation. A pyranometer is a device that measures the total radiant solar energy incident on the analyzed surface per unit time and unit area. The device also allows measurement of the total radiant solar energy reflected from a surface per unit time and unit area, and these data are sufficient to obtain the solar reflectance, as it is the ratio of reflected radiation to incident radiation [67]. In addition to pyranometers and pyrhemometers, solar radiation is also measured using instruments such as solarmeters [68].

A pyrhemometer must be mounted with a device that points the instrument to the Sun throughout the day and measures "direct solar radiation", i.e., the amount of solar energy per unit area and per unit time incident on a plane normal to the Sun's position in the sky, referred to as "direct normal irradiance" or DNI [69]. There are different types of pyrhemometers, and according to Duffie and Beckman (2013) [70], the Abbot silver disc pyrhemometer and the Angstrom compensation pyrhemometer are necessary primary standard instruments. The Eppley normal incidence pyrhemometer (NIP) is a standard instrument used for practical measurements in the US, and the Kipp and Zonen actinometer is widely used in Europe. Both instruments are calibrated according to the primary standard methods. The devices measure the solar radiation beam and the small part of the sky around the Sun.

The solarmeter is a device that can measure solar energy or sunlight in units of W/m^2 , either through windows to check their efficiency or during the installation of solar energy devices. It is designed for environmental monitoring of the sunlight intensity.

Pyrhemometers and pyranometers are standardized according to ISO 9060 [71], which divides them into three classes: the best is designated as the "secondary standard", followed by "first class", and finally, "second class". The standard also distinguishes the thermopile pyrhemometer or pyranometer (as a series-connected thermocouple sensor that converts thermal energy into electrical energy, i.e., measures incident solar radiation by the heat it generates, and a silicon pyranometer has a photoelectric sensor that measures incident solar radiation by the electricity it generates) [72].

The silicon pyranometer is not as uniform and comprehensive in the spectral range. Unlike a thermopile pyranometer, it is not covered by the ISO 9060 standard, and its

calibration methods are not standardized, making direct comparisons with thermopile pyranometers in terms of the accuracy difficult. Therefore, the thermopile pyranometer is highly recommended for measurements with this alternative method. It is worth noting that the World Meteorological Organization (WMO) also classifies pyranometers into three categories: “high quality”, “good quality”, and “moderate quality”. The main difference between this classification and ISO is the requirement for approximately double the spectral response [69,70,72,73]. According to the book *Solar and Infrared Radiation Measurements* by Vignola, Michalsky, and Stoffel (2019) [31], a misalignment of 0.5° in the equipment leveling for solar incidence with a zenith angle of 30° corresponds to an error of 0.1%, and for solar incidence with a zenith angle of 80° , the error increases to 1.2%. Therefore, it is crucial to ensure that the pyranometer is properly leveled and securely mounted.

The measurement range of pyranometers should be between 280 and 2800 nm, with output irradiance values between 0 and 1400 W/m^2 and a one-second response time. Proper use of the pyranometer is recommended, as when facing upward, it measures the total radiant solar energy incident on a horizontal surface per unit time and unit area, and when facing downward, it measures the total radiant solar energy reflected by its surface per unit time and unit area.

This type of pyranometer typically has a double dome to minimize the effects of the internal convection resulting from the pyranometer’s tilt at different angles. Depending on the type of equipment, data from the pyranometer may need to be converted from its analog output to digital by a reading meter, with an accuracy of $\pm 0.5\%$ and a resolution of 1 W/m^2 [73]. The equipment should be placed at least 50 cm away from the surface under analysis, and this distance will influence the sample dimensions. The sample dimensions (diameter or side length) should be at least eight times that distance. Thus, if the sample is circular, it should have a minimum diameter of 4 m, and if it is square, its sides should be at least 4 m. This makes the method suitable for evaluating streets and roofs, among other large surfaces [73].

Finally, it is essential to note that this methodology (ASTM E1918) [74] should only be applied on clear and sunny days, without clouds or fog during measurements, and the sample surfaces should be homogeneous and dry [73,75–79].

3. Case Study

This study was carried out to test and measure the solar radiation in situ with different equipment and its influence on the environmental impact in the Portuguese municipality of Viana do Castelo, located on the northwest coast and NUTS III Alto Minho (Nomenclature of Territorial Units for Statistical Purposes, a hierarchical system for dividing the territory into regions). It is a medium-sized municipality with a population of 85,784 inhabitants living in a total area of $31,902 \text{ km}^2$ (Figure 2).

The demonstration case study consists of a multi-family residential building located in Viana do Castelo, a city in the north of Portugal. The urban context is a historic agglomeration with narrow streets and buildings with an average height of 3 stories. The east, west and north quadrants are consolidated with pre-existing constructions, while the south quadrant is more open, with the presence of notable buildings such as a chapel. The building has a closed block configuration with interior courtyards. Its height is similar to that of the surrounding area. For the case study in question, 4 measurement points were selected (Figure 3), and at each data collection point, 3 pieces of equipment were used to measure the global solar radiation.



Figure 2. Case study area in D. Maria II Street (Viana do Castelo). (A) European context; (B) Alto Minho NUTS III and Municipality of Viana do Castelo; and (C) location of study area.







Figure 3. View of the area of the block chosen as the case study and the respective markings of the data collection points (PC).

The sensors were chosen because they are frequently used in studies of this kind and for reasons of mobility, access, and cost-effectiveness of use (equipment provided by the laboratories of the institution that hosted the study).

In the study area, there was a predominance of buildings with a height of 12 m, flanked by other buildings with a height between 9 and 12 m. The main characteristics of the area adjacent to the measurement equipment, vegetation and traffic are summarized in Table 2.

Table 2. Representation of the study site and its surrounding details.

Photographic Representation of the Study Site and Its Surroundings and Measuring Equipment	Surrounding Vegetation	Surrounding Traffic Routes
 PC1 with northwest solar orientation	A total of 10 deciduous trees with 1 trunk ± 0.30 cm in diameter and 4.00 m high. Foliage when present is ± 8 m in diameter.	Main road with heaviest traffic on the left and secondary road in front of the measuring equipment.
 PC2 with solar orientation south with obstacle	A total of 3 deciduous trees with 1 trunk ± 0.30 cm in diameter and 2.70–3.00 m high. Foliage when present has a diameter of ± 7 m.	Main carriageway with heavier traffic on the left and secondary carriageway in front of the measuring equipment.
 PC3 with east solar orientation	No vegetation around the measuring station.	Secondary road with less car traffic on the left and right is reserved for pedestrians.
 PC4 with solar orientation south without obstacle	A total of 9 evergreen trees, in this case with a trunk with vegetation ± 1 m in diameter and 6–7.00 m high.	Main road with heavier car traffic on the right and secondary road with less traffic in front of the measuring equipment.

To relate equivalent global radiation on sample surfaces, the alternative method E1918A (in situ measurements) was chosen. The choice of the alternative method was due to the ASTM E1918 [74] method requiring large samples, making it difficult to transport and acquire space for placement. The ASTM C1549 [80] method requires more expensive equipment, and the ASTM E903 [81] method can only be used for laboratory measurements.

Therefore, to measure global solar radiation, three solar radiation measurement sensors were chosen—a silicon pyranometer (Skye SP1110 model), a thermopile pyranometer (LP PYRE 02 model) and a solar power meter (SM206-Solar model)—as represented in Table 3.

Table 3. Instruments used for solar radiation measurements.

#	Instrument/Model Name	Measurement	Output Measurement Unit	Accuracy [%]	Range
1	Skye SP11100 SN: 31633	Grad	W/m ²	$\pm 5\%$	1–1100 W/m ²
2	LP PYRE 02 Model	Grad	W/m ²	$\pm 5\%$	0–4000 W/m ²
3	KKMOON SM206	Grad	W/m ²	$\pm 5\%$	1–3999 W/m ²

The measurements took place in real time on 17 February 2023, throughout the day, starting at measurement point PC1 at 9:40 and ending with the last measurement at measurement point PC4 at 18:40. For each measurement/data collection point (PC), 5 measurements were taken throughout the day and were representative of the solar differences of the day (solar time).

As there are no officially recognized standards for determining pyranometer accuracy (manufacturers only provide accuracy estimates), the following practical method is presented when the manufacturer indicates the necessary parameters to estimate the pyranometer measurement accuracy [69].

$$P = \sqrt{(a^2 + b^2 + c^2 + d^2)} \quad (3)$$

where:

P = Accuracy of pyranometer measurements [%];

a = Calibration uncertainty [%];

b = Directional response [%];

c = Temperature response [%];

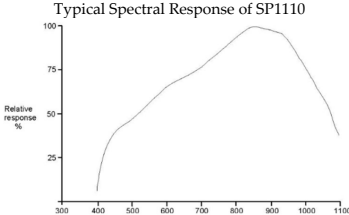
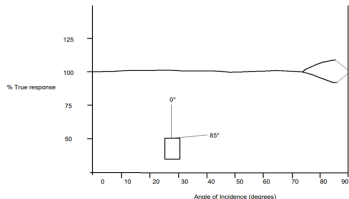
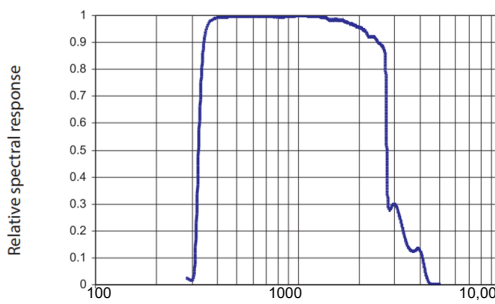
d = Sensitivity change (also called non-stability, depends on the manufacturer and not the pyranometer class) [%].

Therefore, the thermopile pyranometer was used to measure the solar radiation on a uniform sample (the entire building in the case study has the same material coating) with a surface area of approximately 1 m². This technique (referred to as E1918A) was employed to measure the global solar radiation at different in situ measurement points. The other measurement equipment (the silicon pyrometer and the solar meter) do not fulfil all the calculation requirements of Equation (3). Assuming that the accuracy of each piece of equipment is that provided by the suppliers, this is $\pm 5\%$ in all the equipment presented.

Each piece of equipment, with its characteristics, limitations and measurement criteria, is shown in Table 4 and it is easy to understand that the thermopile pyranometer was chosen as the reference sensor because it is the equipment that complies with ISO standards and because it has the most reliable response to the different thermal amplitudes.

The thermopile pyranometer was chosen as it functions linearly, generating more electrical current with a higher measured temperature gradient. That is, if the incident solar radiation doubles, it generates double the electrical current. On the other hand, this sensor also responds directionally, measuring the maximum irradiance when the Sun is directly overhead (zenith angle of 0°) and detecting nothing when the Sun is on the horizon (zenith angle of 90°). Therefore, the pyranometer's electrical signal varies with the cosine of the angle [$\cos(\theta)$] between the Sun and the equipment's normal, one of the parameters influencing pyranometer uncertainties.

Table 4. Measurement instruments: typology, designation, characteristics and performance graphs.

Measuring Instrument	Skye SP11100 SN: 31633	LP PYRE 02 Model	KKMOON SM206
Typology	Silicon Pyranometer	Thermopile Pyranometer	Solar Power Meter
Supplier	CAMPBELL SCIENTIFIC	Delta OHM	Dr. Meter's
Regulatory compliance	Pyranometer Skye SP1110 does not fulfil the ISO 9060 requirements but the World Radiometric Reference standards.	Pyranometer fully complies with ISO 9060 standards and meet the requirements defined by the World Meteorological Organization (WMO).	Solar meter does not comply with the ISO 9060 standard, but fulfills the requirements set by the World Meteorological Organization (WMO).
Equipment Class	Does not fulfil classes	First Class (ISO 9060 standards)	Does not fulfil classes
Characteristics	<p>P = Accuracy of pyranometer measurements [%]. Absolute accuracy $\pm 5\%$ (typically $< \pm 3\%$).</p> <p>a = Calibration uncertainty [%]; output 1 mV per 100 Wm⁻².</p> <p>b = Directional response [%].</p> <p>c = Temperature response [%]. Operating temperature $-35\text{ }^{\circ}\text{C}$ to $+75\text{ }^{\circ}\text{C}$</p> <p>d = Sensitivity change (also called non-stability, depends on the manufacturer and not the not the pyranometer class) [%]. Sensitive to light between 350 nm and 1100 nm.</p>	<p>P = Accuracy of pyranometer measurements [%].</p> <p>a = Calibration uncertainty [%]. ISO 9001 Calibration Report.</p> <p>b = Directional response [%]. Non-linearity $< \pm 1 \%$.</p> <p>c = Temperature response [%]. Operating temperature—$-40\text{--}80\text{ }^{\circ}\text{C}$.</p> <p>d = Sensitivity change (also called non-stability, depends on the manufacturer and not the not the pyranometer class) [%].</p> <p>Typical sensitivity 6 to 12 $\mu\text{V}/(\text{W}/\text{m}^2)$ and $< \pm 1.5 \%$.</p>	<p>P = Accuracy of pyranometer measurements [%]; $\pm 10\text{ W}/\text{m}^2$ [$\pm 5\%$].</p> <p>a = Calibration uncertainty [%].</p> <p>b = Directional response [%].</p> <p>c = Temperature response [%]. Operating temperature—$-10\text{ }^{\circ}\text{C}$ to $60\text{ }^{\circ}\text{C}$.</p> <p>d = Sensitivity change (also called non-stability, depends on the manufacturer and not the pyranometer class) [%].</p>
Performance graphs	<p>Typical Spectral Response of SP1110</p>  <p>Typical Cosine Response Error for SP1110</p>  <p>Typical Cosine Response Error for SP1110</p> <p>Typical Cosine Response Error for SP1110</p>	 <p>Typical spectral response</p>	<p>The equipment in question does not have any studies or tests that would allow a performance or response graph to be drawn up.</p>

4. Results and Discussion

The three solar radiation measurement sensors chosen—a silicon pyranometer (Skye SP1110 model), a thermopile pyranometer (LP PYRE 02 model) and a solar power meter (SM206-Solar model)—to measure point data in real time (17 February 2023) at the same locations (Viana do Castelo City) and in the same conditions (collection points (PC) location, meteorological conditions, same number of hours collection for each point, etc.). Table 5 represents the considerations and values from in situ measurements.

Table 5. Values from the in situ measurements.

Point Control (Measurement)	Measuring Hours (Information Collected on Time)	Silicon Pyranometer (Skye SP1110) (w/m ²)	Thermopile Pyranometer (LP PYRE 02) (w/m ²)	Solar Power Meter (Dr. Meter's) (w/m ²)
PC1	9 h 40	37.3	31.75	42
	11 h 40	41.9	37.9	47.7
	13 h 40	39.5	36.6	48.6
	15 h 40	36.6	34.63	41
	17 h 40	14.8	7.3	17
PC2	10 h 00	68.2	68.4	89
	12 h 00	659	306.8	101.6
	14 h 00	113.9	177.2	136
	16 h 00	54.7	44.8	58
	18 h 00	3.6	0	4
PC3	10 h 20	77.8	71.9	86.7
	12 h 20	679.5	541.7	575.8
	14 h 20	653.6	517.2	920.8
	16 h 20	34.3	31.7	39
	18 h 20	0.66	0	0.6
PC4	10 h 40	652.1	595.9	1118
	12 h 40	679.5	713.3	1108
	14 h 40	500.4	517.2	1033
	16 h 40	31	27.1	40
	18 h 40	0	0	0

As can be seen in Tables 3 and 4, the thermopile pyranometer was chosen as the reference sensor because it is the equipment that complies with the ISO standards and because it provides the most reliable values for the different thermal amplitudes that occur throughout the day in the different measurements and solar hours, as can be seen in the following Figure 4.

It can be analyzed that as the measurements move closer to lunchtime (12:00–14:00), with a greater temperature range, the radiation measurement is also greater and the susceptibility of the equipment to it also suffers depending on the type of sensor. The silicon pyranometer is more sensitive to temperature and light, as it is a sensor calibrated under open sky conditions compared to the reference pyranometers, i.e., according to the World Radiometric Reference.

Due to the different spectral responses of the silicon photocell and thermopiles, to obtain accurate readings, the silicon pyranometer must be used in natural lighting conditions and in different conditions of sun, clouds, etc., which affect the calibration. However,

the reference calibration of the silicon pyranometer in relation to solar energy (300 nm to 3000 nm waveband) is the acceptance band for thermopile pyranometers.

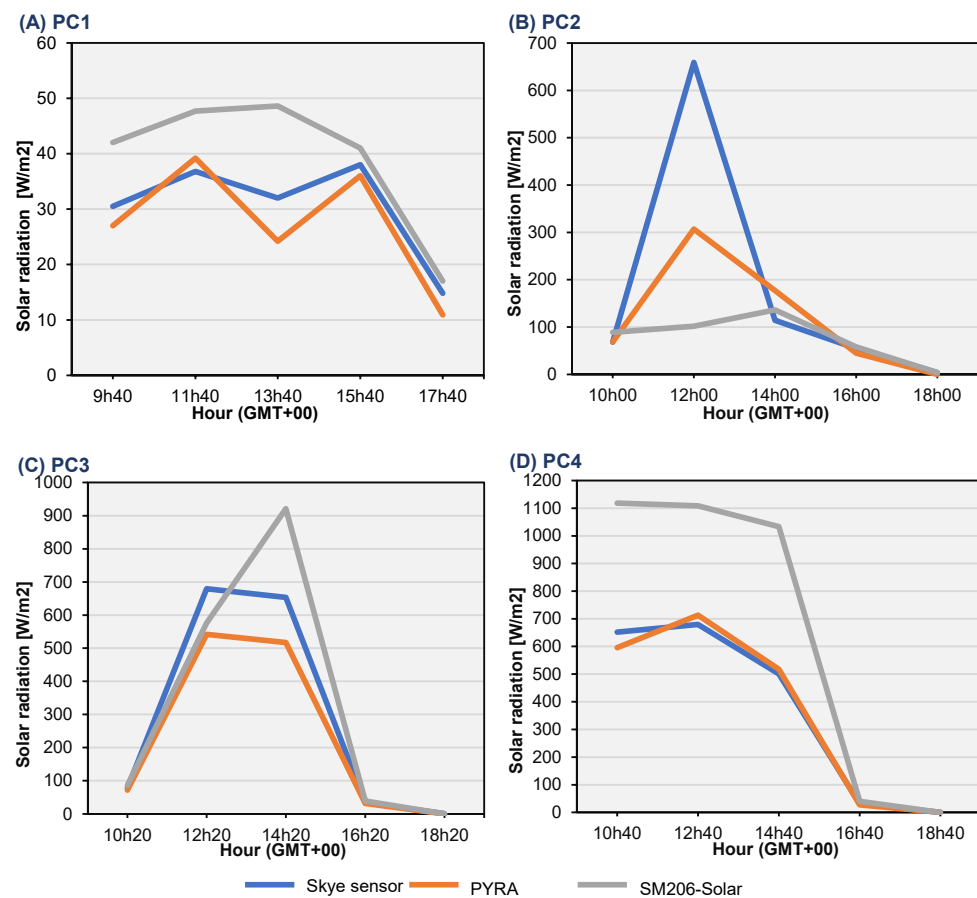


Figure 4. Solar radiation measurements at four data collection points (A) PC1; (B) PC2; (C) PC3; (D) PC4.

In this sense, except for the solar hour (PC2), the behavior of the silicon pyranometer is similar to that of the thermopile pyranometer, as can be seen at data collection points PC1, PC3 and PC4 in Figure 4A,C,D.

On the other hand, the solarmeter, also due to its configuration (see Table 4) and sensitivity to the operating temperature ($-10\text{ }^{\circ}\text{C}$ to $60\text{ }^{\circ}\text{C}$), tends to provide higher values than the thermopile instrument, which is the reference measuring device in this case study.

The pyranometers exhibit values closer to each other compared to the solar meter, as is evident from the various measurements conducted at different times of the day across the four measurement points. This occurrence can be elucidated by Table 3, detailing the factors that impact the equipment's response during radiation measurements.

The three pieces of measuring equipment used in the case study and under the same conditions and with an apparently similar accuracy and range, visible in Table 3, capture and measure different values, as it was possible to verify previously (Figure 4A–D).

Figure 5 shows the relational comparison between the three measuring devices but using the thermopile pyranometer as a reference. As you can see, the silicon pyranometer behaves more assertively and has a slightly higher trend line ($R^2 = 0.911$) than the solar meter ($R^2 = 0.900$).

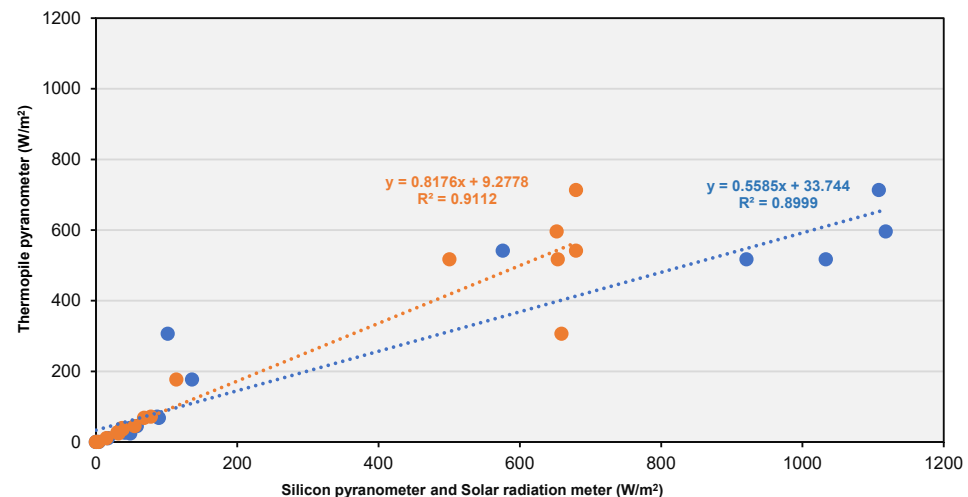


Figure 5. Relational comparison between the thermopile pyranometer and the other two sensors (silicon pyranometer and solar radiation meter). Blue dots represent the relationship between the values measured with the thermopile pyranometer and the solar radiation meter. Orange dots are the relationship between the thermopile pyranometer and the silicon pyranometer.

A comparative analysis of Figure 5 shows that as the solar irradiance increases, the dispersion of the values also increases. As mentioned above, one of the explanations for this phenomenon is the sensitivity of the equipment to increases in the (ambient) temperature.

The proposed methodology aims to reflect the precision of what each piece of equipment measures and the circumstances in which it is considered acceptable—by standards or in response to requests—and the case study aims to exemplify the uncertainties or inaccuracies of the equipment and/or in situ measurements. The overall accuracy and precision of the process are quite complicated as it is necessary to determine which parts are responsible for accuracy errors. The *Guide for Expressing Uncertainty in Measurement* (GUM) defines the difference between an error and uncertainty, wherein the unknowable discrepancy between an idealized “true value” and the observed value is called the measurement error and the measurement uncertainty is the “parameter associated with a measurement result that characterizes the spread of values that could reasonably be attributed to the measurement” [82].

As can be seen by looking at the measurements and the characteristics of the equipment used, in simplistic terms, the trend lines of the measurements throughout the day and at the four measuring points are similar. But if we look at the values obtained in each hour of measurement and at each measurement point, we see that in nominal terms there are fluctuations in the values, especially when we compare the values from the solarmeter with those from the pyranometers. And if we consider the comparison between the silicon pyranometer and the thermopile pyranometer, we can also see the nominal difference.

Equipment errors are inherent to the type of pyranometer used and the calibration applied, and they include zenith error (cosine error), azimuthal error, stability, non-linearity, temperature dependence and spectral response. The highest quality records are obtained with thermopile pyranometers, which are based on the thermoelectric effect.

In the case of thermopiles, as already mentioned, they comply with the ISO 9060/1990 standard [19,21–28,30,31,46,57,74,76–79,83] and the World Meteorological Organization (WMO) which, in addition to establishing quality levels, ensure certain standard standards. The main differences are related to the response time, resolution, stability, linearity and spectral selectivity [84].

5. Conclusions

The Portuguese case study allowed us to verify the need to analyze in depth the parameters of solar radiation that the different equipment on the market measures, in what regards, and what data are obtained from it. As a result, it was found that when estimating solar radiation data for any region, it is possible to include the parameters directly related to solar radiation in that region. In other words, the case study showed that the instruments used to measure the same parameter, regardless of whether they comply with standards and norms with different levels of rigor and equipment quality, are not sufficient to provide accurate data on the solar radiation that reaches a surface in different ways (direct, diffuse or reflected), mainly due to the limitations of each instrument.

The market does not face the problem of lack or insufficiency of data to create models but rather of the fact that much of the data obtained on solar radiation is easily measurable (but generic) and easily accessible, and most of the time the rigor and precision of this data are too inconsistent or volatile. As mentioned above, the different parameters (environmental and ecological) that influence radiation allow and facilitate the study of different regions. However, it is always advantageous to be able to detect the correlation between each input parameter and solar radiation and to extract characteristics and limitations to improve the performance of models (estimates, simulations, etc.) before starting the estimation.

This article addressed solar radiation in situ measurement equipment, including its features, uses, model uncertainty, problem detection, and potential future considerations. Solar radiation is strategic information for a given region when it comes to the possibility of investing in solar energy systems. The information available in advance on the value of solar radiation for a given region is crucial for feasibility studies for that region and is a subject that is increasingly being researched by the academic and business communities. However, it is not practical to install these instruments in all regions due to their high cost, measurement difficulties and calibration problems.

There are alternative measurement options for a future study, considering the previous problematics:

- A cost-effective approach for recording solar radiation involves the use of radiometers utilizing the photovoltaic effect, such as silicon-based photodiodes and solar reference cells. However, these do not meet the quality standards outlined in the ISO 9060/1990 [72] standard due to the limited spectral response of silicon (400–1000 nm).
- Operational errors are independent of the sensor type and encompass various factors, including obstruction by nearby objects, dew, frost, snow, or dust (dirt) covering the pyranometer dome, improper leveling, station interruptions, electric fields near cables, or malfunctioning data loggers, among others.
- Prudent selection of the pyranometer installation site and regular maintenance can mitigate most operational errors.
- Another classification proposed by Zahumenský (2004) [85] distinguishes between random errors, symmetrically distributed around zero; systematic errors, asymmetrically distributed; significant errors primarily caused by device malfunctions and data processing errors; and micrometeorological errors, inconsistencies in ground records concerning surrounding regions.
- All types of errors introduce a certain level of uncertainty into radiation measurements, necessitating quality control (QC).

In completion mode, the accuracy of solar energy production predictions essentially depends on the accuracy of solar irradiance measurements. Vignola et al. (2016) [86] showed that the intensity of solar irradiance has the greatest impact on solar energy production. Research trends have recommended increasing the measurement accuracy of solar irradiance sensors to improve the prediction of solar energy production. Olano et al. (2015) [43] raised several questions regarding the measurement of solar irradiance using a pyranometer. They suggested that the method of pyranometer calibration affects the measurement of solar irradiance. Therefore, calibration must be performed in three types of cloudy conditions to determine the validity of the calibration coefficient for different

types of meteorological conditions. As previously mentioned, this factor, like others, is frequently impossible to establish because testing the three scenarios depends on the time of year the measurement is performed. There are so many variables in measurements and measurement equipment that it is difficult to pragmatically evaluate and obtain data without a margin of error or uncertainty.

Author Contributions: Conceptualization, M.O., P.M. and L.T.S.; methodology, M.O., H.S.L., P.M. and L.T.S.; software, M.O.; validation, M.O., H.S.L., P.M., M.T. and L.T.S.; formal analysis, M.O., H.S.L. and L.T.S.; investigation, M.O., P.M. and L.T.S.; resources, M.O.; data curation, M.O.; writing—original draft preparation, M.O., H.S.L. and L.T.S.; writing—review and editing, M.O., H.S.L., P.M., M.T. and L.T.S. All authors have read and agreed to the published version of the manuscript.

Funding: This work was financed by the Foundation for Science and Technology (FCT) (Grant SFRH/BD/2018)/MCTES through national funds (PIDDAC) under the R&D Centre for Territory, Environment and Construction (CTAC), under reference UID/04047/2020, and the Landscapes, Heritage and Territory Laboratory (Lab2PT) Center of Design and Technology (DeTech).

Data Availability Statement: The data presented in this study are available on request from the corresponding author.

Acknowledgments: The authors gratefully acknowledge the funding support of the Foundation for Science and Technology (FCT) and the Centre for Territory, Environment and Construction (CTAC).

Conflicts of Interest: The authors declare no conflicts of interest.

References

- Besharat, F.; Dehghan, A.A.; Faghih, A.R. Empirical models for estimating global solar radiation: A review and case study. *Renew. Sustain. Energy Rev.* **2013**, *21*, 798–821. [\[CrossRef\]](#)
- Khatib, T.; Mohamed, A.; Sopian, K. A review of solar energy modeling techniques. *Renew. Sustain. Energy Rev.* **2012**, *16*, 2864–2869. [\[CrossRef\]](#)
- Qiu, R.; Li, L.; Wu, L.; Agathokleous, E.; Liu, C.; Zhang, B.; Luo, Y.; Sun, S. Modeling daily global solar radiation using only temperature data: Past, development, and future. *Renew. Sustain. Energy Rev.* **2022**, *163*, 112511. [\[CrossRef\]](#)
- Guerrou, M.; Melgani, F.; Gairaa, K.; Mekhalfi, M.L. A comprehensive review of hybrid models for solar radiation forecasting. *J. Clean. Prod.* **2020**, *258*, 120357. [\[CrossRef\]](#)
- Gürel, A.E.; Ağbulut, Ü.; Bakır, H.; Ergün, A.; Yıldız, G. A state of art review on estimation of solar radiation with various models. *Heliyon* **2023**, *9*, e13167. [\[CrossRef\]](#)
- Park, J.K.; Das, A.; Park, J.H. A new approach to estimate the spatial distribution of solar radiation using topographic factor and sunshine duration in South Korea. *Energy Convers. Manag.* **2015**, *101*, 30–39. [\[CrossRef\]](#)
- Matejcek, L. Solar Energy: Estimates of Energy Potential and Environmental Issues. In *Assessment of Energy Sources Using GIS*; Springer: Berlin/Heidelberg, Germany, 2017; pp. 221–244. [\[CrossRef\]](#)
- Ritchie, H.; Roser, M.; Rosado, P. Renewable Energy. Our World Data. 2023. Available online: <https://ourworldindata.org/renewable-energy> (accessed on 12 December 2023).
- WCED. Special Working Session: World commission on environment and development. *Our Common Future* **1987**, *17*, 1–91.
- Ağbulut, Ü.; Gürel, A.E.; Biçen, Y. Prediction of daily global solar radiation using different machine learning algorithms: Evaluation and comparison. *Renew. Sustain. Energy Rev.* **2021**, *135*, 110114. [\[CrossRef\]](#)
- Ceylan, I.; Gürel, A.E.; Demircan, H.; Aksu, B. Cooling of a photovoltaic module with temperature controlled solar collector. *Energy Build.* **2014**, *72*, 96–101. [\[CrossRef\]](#)
- Al-Ghezi, M.K.; Ahmed, R.T.; Chaichan, M.T. The Influence of Temperature and Irradiance on Performance of the photovoltaic panel in the Middle of Iraq. *Int. J. Renew. Energy Dev.* **2022**, *11*, 501–513. [\[CrossRef\]](#)
- Pandey, A.; Pandey, P.; Tumuluru, J.S. Solar Energy Production in India and Commonly Used Technologies—An Overview. *Energies* **2022**, *15*, 500. [\[CrossRef\]](#)
- Obiora, C.N.; Ali, A.; Hasan, A.N. Forecasting Hourly Solar Irradiance Using Long Short-Term Memory (LSTM) Network. In Proceedings of the 11th International Renewable Energy Congress, IREC 2020, Hammamet, Tunisia, 29–31 October 2020. [\[CrossRef\]](#)
- Diagne, M.; David, M.; Lauret, P.; Boland, J.; Schmutz, N. Review of solar irradiance forecasting methods and a proposition for small-scale insular grids. *Renew. Sustain. Energy Rev.* **2013**, *27*, 65–76. [\[CrossRef\]](#)
- Jendritzky, G. Selected questions of topical interest in human bioclimatology. *Int. J. Biometeorol.* **1991**, *35*, 139–150. [\[CrossRef\]](#) [\[PubMed\]](#)
- Matzarakis, A.; Mayer, H.; Rutz, F. Radiation and thermal comfort. In Proceedings of the 6th Hellenic Conference in Meteorology, Climatology and Atmospheric Physics, Ioannina, Greece, 25–28 of September 2002; pp. 739–744.

18. Matzarakis, A.; Rutz, F.; Mayer, H. Modelling radiation fluxes in simple and complex environments—Application of the RayMan model. *Int. J. Biometeorol.* **2007**, *51*, 323–334. [\[CrossRef\]](#)
19. Nollas, F.M.; Salazar, G.A.; Gueymard, C.A. Quality control procedure for 1-minute pyranometric measurements of global and shadowband-based diffuse solar irradiance. *Renew. Energy* **2023**, *202*, 40–55. [\[CrossRef\]](#)
20. Lorenz, E.; Guthke, P.; Dittmann, A.; Holland, N.; Herzberg, W.; Karalus, S.; Müller, B.; Braun, C.; Heydenreich, W.; Saint-Drenan, Y.M. High resolution measurement network of global horizontal and tilted solar irradiance in southern Germany with a new quality control scheme. *Sol. Energy* **2022**, *231*, 593–606. [\[CrossRef\]](#)
21. Mudike, R.; Barbate, I.; Tripathi, A.K.; Nikhil, P.G.; Banerjee, C. Calibration of solar radiometers with traceability to the world radiometric reference using an absolute cavity radiometer. *Measurement* **2021**, *179*, 109475. [\[CrossRef\]](#)
22. Mohammad, S.T.; Al-Kayiem, H.H.; Aurybi, M.A.; Khelif, A.K. Measurement of global and direct normal solar energy radiation in Seri Iskandar and comparison with other cities of Malaysia. *Case Stud. Therm. Eng.* **2020**, *18*, 100591. [\[CrossRef\]](#)
23. Moiz, S.A.; Alahmadi, A.N.M.; Aljohani, A.J. Design of silicon nanowire array for PEDOT: PSS-silicon nanowire-based hybrid solar cell. *Energies* **2020**, *13*, 3797. [\[CrossRef\]](#)
24. Lillo-Bravo, I.; Larrañeta, M.; Núñez-Ortega, E.; González-Galván, R. Simplified model to correct thermopile pyranometer solar radiation measurements for photovoltaic module yield estimation. *Renew. Energy* **2020**, *146*, 1486–1497. [\[CrossRef\]](#)
25. Palo-Tejada, E.; Campos-Falcon, V.; Merma, M.; Huanca, E. Low-cost data logging device to measure irradiance based on a Peltier cell and artificial neural networks. *J. Phys.* **2020**, *1433*, 12008. [\[CrossRef\]](#)
26. John, C.I.; Mahmood, M.K.; Abubakar, B.; Lawal, O.K.; Nakorji, H.U.; Kabir, S.D. Design and Implementation of an Electronic Pyranometer. *IOSR J. Electr. Electron. Eng. (IOSR-JEEE) E-ISSN* **2019**, *14*, 1676–2278.
27. Azouzoute, A.; Merrouni, A.A.; Bennouna, E.G.; Gennioui, A. Accuracy Measurement of Pyranometer vs Reference cell for PV resource assessment. *Energy Procedia* **2019**, *157*, 1202–1209. [\[CrossRef\]](#)
28. Tohsing, K.; Phaisathit, D.; Pattarapanitchai, S.; Masiri, I.; Buntoung, S.; Aumporn, O.; Wattan, R. A development of a low-cost pyranometer for measuring broadband solar radiation. *J. Phys.* **2019**, *1380*, 12045. [\[CrossRef\]](#)
29. Osinowo, M.O.; Willoughby, A.A.; Ewetumo, T.; Kolawole, L.B. Development of a Low-Cost Pyrometer using Locally Sourced Materials. *Int. J. Sci. Res. Dev.* **2019**, *7*.
30. Rus-Casas, C.; Hontoria, L.; Fernández-Carrasco, J.I.; Jiménez-Castillo, G.; Muñoz-Rodríguez, F. Development of a Utility Model for the Measurement of Global Radiation in Photovoltaic Applications in the Internet of Things (IoT). *Electronics* **2019**, *8*, 304. [\[CrossRef\]](#)
31. Vignola, F.; Michalsky, J.; Stoffel, T. *Solar and Infrared Radiation Measurements*, 2nd ed.; CRC Press: Boca Raton, FL, USA, 2019; pp. 1–494. [\[CrossRef\]](#)
32. de Barros, R.C.; Callegari, J.M.S.; do Carmo Mendonça, D.; Amorim, W.C.S.; Silva, M.P.; Pereira, H.A. Low-cost solar irradiance meter using LDR sensors. In Proceedings of the 13th IEEE International Conference on Industry Applications (INDUSCON), Sao Paulo, Brazil, 12–14 November 2018; pp. 72–79.
33. Avallone, E.; Mioralli, P.C.; Scalón, V.L.; Padilha, A.; Oliveira, S.d.R. Thermal pyranometer using the open hardware arduino platform. *Int. J. Thermodyn.* **2018**, *21*, 1–5. [\[CrossRef\]](#)
34. López-Lapeña, O.; Pallas-Areny, R. Solar energy radiation measurement with a low-power solar energy harvester. *Comput. Electron. Agric.* **2018**, *151*, 150–155. [\[CrossRef\]](#)
35. Awasthi, J.; Poudyal, K.N. Estimation of Global Solar Radiation Using Empirical Model on Meteorological Parameters at Simara Airport, Bara, Nepal. *J. Inst. Eng.* **2018**, *14*, 143–150. [\[CrossRef\]](#)
36. Vignola, F.; Peterson, J.; Kessler, R.; Dooraghi, M.; Sengupta, M.; Mavromatakis, F. Evaluation of photodiode-based pyranometers and reference solar cells on a two-axis tracking system. In Proceedings of the IEEE 7th World Conference on Photovoltaic Energy Conversion (WCPEC) (A Joint Conference of 45th IEEE PVSC, 28th PVSEC & 34th EU PVSEC), Waikoloa, HI, USA, 10–15 June 2018; pp. 2376–2381.
37. Orsetti, C.; Muttillio, M.; Parente, F.R.; Pantoli, L.; Stornelli, V.; Ferri, G. Reliable and inexpensive solar irradiance measurement system design. *Procedia Eng.* **2016**, *168*, 1767–1770. [\[CrossRef\]](#)
38. Michalsky, J.J.; Kutchenreiter, M.; Long, C.N. Significant improvements in pyranometer nighttime offsets using high-flow DC ventilation. *J. Atmos. Ocean. Technol.* **2017**, *34*, 1323–1332. [\[CrossRef\]](#)
39. Parthasarathy, S.; Anandkumar, N.V. Development of Low Cost Data Acquisition System for Photo Voltaic Systems. *Int. J. Innov. Res. Sci. Eng. Technol.* **2016**, *5*, 12850–12856.
40. Chaipapinunt, S.; Ruttanasupa, P.; Ariyapoonpong, V.; Duanmeesook, K. A shadow-ring device for measuring diffuse solar radiation on a vertical surface in a tropical zone. *Sol. Energy* **2016**, *136*, 629–638. [\[CrossRef\]](#)
41. Agawa, Y.Y.; Ibrahim, S.B. Development of micro controller-based monitoring system for a stand-alone photovoltaic system. *Niger. J. Technol.* **2016**, *35*, 904–911. [\[CrossRef\]](#)
42. Nwankwo, S.; Nnabuchi, M. Global solar radiation measurement in Abakaliki Ebonyi state Nigeria using locally made pyranometer. *Int. J. Energy Environ. Res.* **2015**, *3*, 47–54.
43. Olano, X.; Sallaberry, F.; García De Jalón, A.; Gastón, M. The influence of sky conditions on the standardized calibration of pyranometers and on the measurement of global solar irradiation. *Sol. Energy* **2015**, *121*, 116–122. [\[CrossRef\]](#)
44. Srikrishnan, V.; Young, G.S.; Witmer, L.T.; Brownson, J.R.S. Using multi-pyranometer arrays and neural networks to estimate direct normal irradiance. *Sol. Energy* **2015**, *119*, 531–542. [\[CrossRef\]](#)

45. Dumitrescu, A.L.; Paulescu, M.; Ercuta, A. A Solid State Pyranometer. *Ann. West Univ. Timis.-Phys.* **2015**, *58*, 56–63. [CrossRef]
46. Menyhart, L.; Anda, A.; Nagy, Z. A new method for checking the leveling of pyranometers. *Solar Energy* **2015**, *120*, 25–34. [CrossRef]
47. Fuentes, M.; Vivar, M.; Burgos, J.M.; Aguilera, J.; Vacas, J.A. Design of an accurate, low-cost autonomous data logger for PV system monitoring using ArduinoTM that complies with IEC standards. *Sol. Energy Mater. Sol. Cells* **2014**, *130*, 529–543. [CrossRef]
48. Daniel, A.A.; Odinakachi, E.E. Design, Construction and Calibration of a Solar Radiation Measuring Meter. *Rev. Adv. Phys. Theor. Appl.* **2014**, *1*, 1–8. [CrossRef]
49. Design of a Low-Cost Sensor for Solar Irradiance. 2013. Available online: <http://oceanoptics.com/> (accessed on 22 May 2024).
50. Hafid, A.A.; Meddah, K.; Attari, M.; Remram, Y. A Thermopile Based Pyranometer for Large Spectrum Sunlight Measurement. In Proceedings of the International Conference on Embedded Systems in Telecommunications and Instrumentation (ICESTI'14), Annaba, Algeria, 27 October 2014.
51. Baltazar, J.-C.; Sun, Y.; Haberl, J. Improved Methodology to Measure Normal Incident Solar Radiation with a Multi-pyranometer Array. *Energy Procedia* **2014**, *57*, 1211–1219. [CrossRef]
52. Geuder, N.; Affolter, R.; Kraas, B.; Wilbert, S. Long-term Behavior, Accuracy and Drift of LI-200 Pyranometers as Radiation Sensors in Rotating Shadowband Irradiometers (RSI). *Energy Procedia* **2014**, *49*, 2330–2339. [CrossRef]
53. Patil, A.; Haria, K.; Pashte, P. Photodiode based pyranometer. *Int. J. Adv. Sci. Eng. Technol.* **2013**, *1*, 29–33.
54. Awasthi, S.; Mor, P. Web based measurement system for solar radiation. *Int. J. Adv. Comput. Res.* **2012**, *2*, 101.
55. Nwankwo, S.N.; Nnabuchi, M.N.; Ekpe, J.E. Construction and Characterization of a Pyranometer Using Locally Available Materials for Global Solar Radiation Measurement. *Asian Transact. Basic Appl. Sci.* **2012**, *26*, 26–33.
56. Medugu, D.W.; Burari, F.W.; Abdulazeez, A.A. Construction of a reliable model pyranometer for irradiance measurements. *Afr. J. Biotechnol.* **2010**, *9*, 1719–1725. [CrossRef]
57. Macome, M.A.; Cuamba, B.; Pillay, S.; Lovseth, J. Design, Construction and Characterization of a Multiple Sensors Solar Radiation Detector for Ises. 2009. Available online: https://energypedia.info/images/3/30/EN-DESIGN_CONSTRUCTION_AND_CHARACTERIZATION_OF_A_MULTIPLE_SENSORS_SOLAR_RADIATION_DETECTOR_FOR_ISES_2009-M.A._Macome1_et_al.pdf (accessed on 22 May 2024).
58. Martínez, M.A.; Andújar, J.M.; Enríque, J.M. A new and inexpensive pyranometer for the visible spectral range. *Sensors* **2009**, *9*, 4615–4634. [CrossRef]
59. Gueymard, C.A.; Myers, D.R. Evaluation of conventional and high-performance routine solar radiation measurements for improved solar resource, climatological trends, and radiative modeling. *Sol. Energy* **2009**, *83*, 171–185. [CrossRef]
60. Lester, A.; Myers, D.R. A method for improving global pyranometer measurements by modeling responsivity functions. *Sol. Energy* **2006**, *80*, 322–331. [CrossRef]
61. Onwuala, W.I.; Okonkwo, A.P. Design, Construction and Evaluation of a Pyranometer for Radiation Measurement. *Sci. Forum J. Pure Appl.* **2002**, *5*, 234–240.
62. Beaubien, D.J.; Bisberg, A.; Beaubien, A.F. Investigations in pyranometer design. *J. Atmos. Ocean. Technol.* **1998**, *15*, 677–686. [CrossRef]
63. Soulayman, S.S.; Daudé, N. A correction method for solar radiation measurements made using non-calibrated Eppley-type and Robitzsch-type pyranometers. *Appl. Energy* **1995**, *52*, 125–132. [CrossRef]
64. Wang, F.; Xuan, Z.; Zhen, Z.; Li, Y.; Li, K.; Zhao, L.; Shafie-khah, M.; Catalão, J.P. A minutely solar irradiance forecasting method based on real-time sky image-irradiance mapping model. *Energy Convers. Manag.* **2020**, *220*, 113075. [CrossRef]
65. Ameen, B.; Balzter, H.; Jarvis, C.; Wheeler, J. Modelling Hourly Global Horizontal Irradiance from Satellite-Derived Datasets and Climate Variables as New Inputs with Artificial Neural Networks. *Energies* **2019**, *12*, 148. [CrossRef]
66. Mohanty, S.; Patra, P.K.; Sahoo, S.S.; Mohanty, A. Forecasting of solar energy with application for a growing economy like India: Survey and implication. *Renew. Sustain. Energy Rev.* **2017**, *78*, 539–553. [CrossRef]
67. Harrison, D.C.; Seah, W.K.G.; Rayudu, R.K. Coverage preservation in energy harvesting wireless sensor networks for rare events. In Proceedings of the 2015 IEEE 40th Conference on Local Computer Networks (LCN), Clearwater Beach, FL, USA, 26–29 October 2015; pp. 181–184.
68. Karaman, Ö.A.; Tanyıldızı Ağır, T.; Arsel, İ. Estimation of solar radiation using modern methods. *Alex. Eng. J.* **2021**, *60*, 2447–2455. [CrossRef]
69. Hukseflux. What Is a Pyrheliometer? | Hukseflux. Available online: <https://www.hukseflux.com/applications/solar-energy-pv-system-performance-monitoring/what-is-a-pyrheliometer> (accessed on 24 November 2023).
70. Duffie, J.A.; Beckman, W.A. *Solar Engineering of Thermal Processes*; John Wiley & Sons, Inc.: Hoboken, NJ, USA, 2013. [CrossRef]
71. The US Solar Institute. Pyranometer. The US Solar Institute. Available online: <https://www.myussi.com/glossary/pyranometer/> (accessed on 12 December 2023).
72. ISO 9060:1990(en); Solar Energy—Specification and Classification of Instruments for Measuring Hemispherical Solar and Direct Solar Radiation. ISO: Geneva, Switzerland, 1990.
73. ASTM. G183 Standard Practice for Field Use of Pyranometers, Pyrheliometers and UV Radiometers. 2023. Available online: <https://www.astm.org/g0183-15.html> (accessed on 25 May 2023).
74. ASTM E1918; Standard Test Method for Measuring Solar Reflectance of Horizontal and Low-Sloped Surfaces in the Field 1. ASTM: West Conshohocken, PA, USA, 2021. [CrossRef]

75. Levinson, R.; Akbari, H.; Berdahl, P. Measuring solar reflectance—Part I: Defining a metric that accurately predicts solar heat gain. *Sol. Energy* **2010**, *84*, 1717–1744. [[CrossRef](#)]
76. Levinson, R.; Akbari, H.; Berdahl, P. Measuring solar reflectance—Part II: Review of practical methods. *Sol. Energy* **2010**, *84*, 1745–1759. [[CrossRef](#)]
77. Akbari, H.; Levinson, R.; Stern, S. Procedure for measuring the solar reflectance of flat or curved roofing assemblies. *Sol. Energy* **2008**, *82*, 648–655. [[CrossRef](#)]
78. Levinson, R.; Egolf, M.; Chen, S.; Berdahl, P. Experimental comparison of pyranometer, reflectometer, and spectrophotometer methods for the measurement of roofing product albedo. *Sol. Energy* **2020**, *206*, 826–847. [[CrossRef](#)]
79. ASTM E1918-16; Standard Test Method for Measuring Solar Reflectance of Horizontal and Low-Slope Surface in the Field. ASTM International: West Conshohocken, PA, USA, 2016.
80. C1549-04; Standard Test Method for Determination of Solar Reflectance near Ambient Temperature Using a Portable Solar Reflectometer. ASTM International: West Conshohocken, PA, USA, 2002.
81. ASTM E903-20; Standard Test Method for Solar Absorptance, Reflectance, and Transmittance of Materials Using Integrating Spheres. ASTM International: West Conshohocken, PA, USA, 2020.
82. JCGM 100:2008(E); Evaluation of Measurement Data—Guide to the Expression of Uncertainty in Measurement. International Organization for Standardization (ISO): Geneva, Switzerland, 2008. [[CrossRef](#)]
83. Niewianda, A.; Heidt, F.D. Sombrero: A PC-Tool To Calculate Shadows On Arbitrarily Oriented Surfaces. *Sol. Energy* **1996**, *58*, 253–263. [[CrossRef](#)]
84. Paulescu, M.; Paulescu, E.; Gravila, P.; Badescu, V. *Weather Modeling and Forecasting of PV Systems Operation*; Green Energy and Technology; Springer: Berlin/Heidelberg, Germany, 2013; Volume 103.
85. Zahumensky, I. Guidelines on Quality Control Procedures for Data from Automatic Weather Stations. 2004. Available online: https://www.researchgate.net/publication/228826920_Guidelines_on_Quality_Control_Procedures_for_Data_from_Automatic_Weather_Stations%3E (accessed on 29 January 2024).
86. Vignola, F.; Derocher, Z.; Peterson, J.; Vuilleumier, L.; Félix, C.; Gröbner, J.; Kouremeti, N. Effects of changing spectral radiation distribution on the performance of photodiode pyranometers. *Sol. Energy* **2016**, *129*, 224–235. [[CrossRef](#)]

Disclaimer/Publisher’s Note: The statements, opinions and data contained in all publications are solely those of the individual author(s) and contributor(s) and not of MDPI and/or the editor(s). MDPI and/or the editor(s) disclaim responsibility for any injury to people or property resulting from any ideas, methods, instructions or products referred to in the content.